Resistance towards monensin is proposed to be acquired in a *Toxoplasma gondii* model by reduced invasion and egress activities, in addition to increased intracellular replication

AHMED THABET[1], JOHANNES SCHMIDT[2], SVEN BAUMANN[2,3], WALTHER HONSCHA[4], MARTIN VON BERGEN[2,5,6], ARWID DAUGSCHIES[1,7] *and* BERIT BANGOURA[1,8]*

[1] *Institute of Parasitology, Faculty of Veterinary Medicine, Centre for Infectious Diseases, University of Leipzig, Leipzig, Germany*
[2] *Department of Molecular Systems Biology, Helmholtz-Centre for Environmental Research – UFZ, Leipzig, Germany*
[3] *Institute of Pharmacy, Faculty of Biosciences, Pharmacy and Psychology, University of Leipzig, Leipzig, Germany*
[4] *Institute of Pharmacology, Pharmacy and Toxicology, Faculty of Veterinary Medicine, University of Leipzig, Leipzig, Germany*
[5] *Institute of Biochemistry, Faculty of Biosciences, Pharmacy and Psychology, University of Leipzig, Leipzig, Germany*
[6] *Department of Chemistry and Bioscience, Center for Microbial Communities, University of Aalborg, Aalborg East, Denmark*
[7] *Albrecht-Daniel-Thaer-Institute, Leipzig, Germany*
[8] *University of Wyoming, Department of Veterinary Sciences, Laramie, WY, USA*

(*Received 21 February 2017; revised 26 May 2017; accepted 31 July 2017; first published online 5 September 2017*)

SUMMARY

Monensin (Mon) is an anticoccidial polyether ionophore widely used to control coccidiosis. The extensive use of polyether ionophores on poultry farms resulted in widespread resistance, but the underlying resistance mechanisms are unknown in detail. For analysing the mode of action by which resistance against polyether ionophores is obtained, we induced *in vitro* Mon resistance in *Toxoplasma gondii*-RH strain (MonR-RH) and compared it with the sensitive parental strain (Sen-RH). The proteome assessment of MonR-RH and Sen-RH strains was obtained after isotopic labelling using stable isotope labelling by amino acid in cell culture. Relative proteomic quantification between resistant and sensitive strains was performed using liquid chromatography-mass spectrometry/mass spectrometry. Overall, 1024 proteins were quantified and 52 proteins of them were regulated. The bioinformatic analysis revealed regulation of cytoskeletal and transmembrane proteins being involved in transport mechanisms, metal ion-binding and invasion. During invasion, actin and microneme protein 8 (MIC8) are seem to be important for conoid extrusion and forming moving junction with host cells, respectively. Actin was significantly upregulated, while MIC8 was downregulated, which indicate an invasion reduction in the resistant strain. Resistance against Mon is not a simple process but it involves reduced invasion and egress activity of *T. gondii* tachyzoites while intracellular replication is enhanced.

Key words: *Toxoplasma gondii*, stable isotope labelling by amino acid in cell culture, monensin, resistance mechanism, SILAC.

INTRODUCTION

Polyether ionophores are a class of anticoccidial and antimicrobial agents that can bind with cationic metal ions, i.e. sodium, and facilitate its transport across cellular membranes presumably by modifying cellular membrane permeability (Kevin *et al*. 2009). Monensin (Mon), a sodium polyether ionophore, is considered the most frequently used polyether ionophore to control coccidiosis (Chapman *et al*. 2010) and is highly effective against cysts of *Toxoplasma gondii* (Couzinet *et al*. 2000).

Development of resistance against polyether ionophores has been documented in all compounds with market authorization (Stephan *et al*. 1997; Peek and Landman, 2003). Mechanisms of resistance were studied in *Eimeria tenella* against polyether ionophores using cDNA array (Chen *et al*. 2008). It was found that genes involved in cytoskeletal rearrangments and energy metabolism were upregulated in Mon-resistant compared with its parental sensitive strain. On the other hand, genes related to invasion were downregulated in maduramicin-resistant strains.

Toxoplasma gondii is a worldwide-distributed apicomplexan parasite that is capable to infect many warm-blooded animals including man as intermediate or erroneous host whereas felines are the only definite hosts (Dubey *et al*. 2011; McFarland *et al*. 2016). *Toxoplasma gondii* shares certain biological features including their sensitivity towards Mon with other apicomplexan members. Asexual stage of type I *T. gondii* RH strain (tachyzoites) can be

* Corresponding author: Department of Veterinary Sciences, WSVL, 1174 Snowy Range Rd, 82070 Laramie, WY, USA. E-mail: bbangour@uwyo.edu

doi:10.1017/S0031182017001512

grown continuously in cell culture and do not form cysts (Mavin *et al*. 2004). Continuous *in vitro* culture is, therefore, easy to maintain, reliable and can provide a tremendous amount of tachyzoites. Human foreskin fibroblast (HFF) cells promote effective and rapid tachyzoite replication (Wu *et al*. 2009). Therefore, induction of *in vitro* resistance in *T. gondii* tachyzoites against Mon could be used as an approach for better understanding the mechanisms of resistance development in apicomplexan parasites (Ricketts and Pfefferkorn, 1993). A novel mode of action was suggested for mechanism of Mon resistance in *T. gondii*, in which MutS Homolog (MSH-1) was involved in induction of mitochondrial stress and disruption. Moreover, disruption of MSH-1 resulted in reduced sensitivity towards Mon (Garrison and Arrizabalaga, 2009).

Mass spectrometry-based quantitative proteomics can provide insights into protein expression of biological systems at certain conditions by identification and relative quantification of thousands of proteins. Hence, it has been shown to be a valuable tool to improve our understanding of biological processes including mechanisms of drug resistance (Ong and Mann, 2005). Stable isotope labelling by amino acid in cell culture (SILAC) has been applied extensively for relative quantification in studying complex biological systems. SILAC was applied successfully in *T. gondii* to study mechanisms of vital biological processes such as invasion and egress (Heaslip *et al*. 2010; Treeck *et al*. 2014). The ability of *T. gondii* tachyzoites to continuously grow in cell cultures enables the efficient differential labelling of strains using heavy and light amino acids. After mixing of heavy and light-labelled samples the analysis of digested peptides mixtures using liquid chromatography-mass spectrometry/mass spectrometry (LC-MS/MS) provides a robust and accurate detection of strain-specific differences in proteomic profiles of labelled parasites.

In this study, we induced resistance in *T. gondii* RH strain against Mon. Proteins that directly interfere with mechanisms of Mon resistance were searched through comparative quantification of Mon-resistant and -sensitive strains using SILAC labelling.

MATERIALS AND METHODS

Induction of resistance in T. gondii *(RH strain) against Mon*

Parasite and cell culture conditions. A mutant, Mon-resistant RH strain of *T. gondii* (MonR-RH) was generated *in vitro* from a Mon-sensitive parental RH strain (Sen-RH) as described before (Ricketts and Pfefferkorn, 1993). Low-passage HFF cells (ATCC®SCRC-1041) were grown in tissue-culture dishes in Dulbecco's modified Eagle's medium (DMEM, with high glucose and L-glutamine, supplemented with 10% newborn calf serum; Gibco, Germany) at 37 °C and 5% CO_2 to obtain semi-confluent monolayers. During *T. gondii* tachyzoite infection, 2% newborn calf serum was used and antibiotics were added (penicillin, 100 U mL^{-1}; streptomycin, 100 $\mu g\ mL^{-1}$ and amphotericin-B, 0·25 $\mu g\ mL^{-1}$; GE Healthcare, Munich, Germany). Tachyzoites were obtained from destroyed HFF cells after 148 h post-infection (p.i.), the attached parasites were detached using a 25-gauge needle and used to re-infect fresh HFF cells. DMEM was changed every 72 h during the experiment.

Dose determination of Mon. Tachyzoites of parental Sen-RH were incubated with various concentrations of Mon to estimate the initial concentration to be used. Minimum inhibitory concentration (MIC_{50}) was stated as the lowest concentration of Mon that will inhibit tachyzoite replication by at least 50% compared with infected non-treated controls. To determine MIC_{50} for RH strain tachyzoites, DMEM was supplemented with Mon at various concentrations ranging from 0·25 to 32·0 ng mL^{-1}. HFF cells were grown in 24-well tissue culture plates and after reaching more than 80% confluence, $2{\cdot}5 \times 10^4$ tachyzoites were added and the cultures were further incubated for 72 h at 37 °C. Trypsin-versene (Lonza, Thermo Scientific, Germany) was added to infected HFF cells containing intracellular tachyzoites. DMEM containing extracellular tachyzoites and harvested infected HFF cells were centrifuged (2778 ***g***, 10 min) and the pellet was reconstituted in 200 μL phosphate-buffered saline (PBS). For DNA extraction, QIAamp® DNA Mini Kit (Qiagen, Hilden, Germany) was used according to the manufacturer's instructions (blood and body fluid spin protocol). Each assay was performed in quadruplicate.

Real-time quantitative PCR (qPCR, TaqMan) based on the 529-bp repeat element specific for *T. gondii* was used to determine the number of tachyzoites in each replicate of the cell cultures as described before (Edvinsson *et al*. 2006). Standard curve for quantification and calculation of amplification's efficacy was conducted by diluting DNA from known tachyzoites number of *T. gondii* RH strain serially (starting DNA concentration: 5×10^6 tachyzoites/5 μL). No-template controls and no-amplification control were included. The mean value for three replicates with an acceptable standard deviation of <0·5 was calculated.

The dose–response curve between log (Mon concentrations; $\mu g\ mL^{-1}$) and % of inhibition in Sen-RH replication was plotted to estimate MIC_{50} of Mon on Sen-RH.

Resistance induction. To produce MonR-RH, $1{\cdot}0 \times 10^6$ tachyzoites of the sensitive parent strain were continuously grown HFF monolayers in

https://doi.org/10.1017/S0031182017001512 Published online by Cambridge University Press

Mon-containing media starting with the pre-determined concentration of 0·5 ng mL^{-1}. Harvesting and splitting of newly produced tachyzoites was performed as described before. Mon concentration was increased by 0·1 ng mL^{-1} after a robust growing of tachyzoites was noticed by their ability to damage most of HFF cells after 148 h. Moreover, ability of tachyzoites to grow in the presence of the increased Mon concentration was assessed using qPCR to assure their ability to replicate after 148 h p.i. Aliquots of newly produced RH tachyzoites were stored in liquid nitrogen every five successful passages. Cultivation in the presence of Mon was continued for more than 8 months. Comparison between Sen-RH and MonR-RH was performed by cultivating $2{\cdot}5 \times 10^4$ tachyzoites of each strain in HFF cells for 96 h at 37 °C. DNA extraction and qPCR conditions were done as described above. Comparing MonR-RH and Sen-RH to produce tachyzoites in the absence or presence of different concentrations of Mon (0·5–5 ng mL^{-1}) was performed by comparing growth rates and calculating per cent (%) of replication of both strains (Fig. 1a).

$$\%\,\text{of replication} = \frac{\text{no. of tachyzoites in Mon} - \text{treated replicates}}{\text{no. of tachyzoites in infected, non} - \text{treated control}}$$

SILAC experiment

Labelling. HFF cells were split twice sequentially in a ratio 1 : 4 after reaching 80% confluence in the presence of no tachyzoites to assure that heavy stable isotopes of essential amino acids have been introduced to all newly synthesized proteins and the complete cellular proteome was incorporated with these isotopes. Sen-RH and MonR-RH were labelled as previously described (Heaslip *et al*. 2010). Briefly, HFF cells were grown either in heavy (146 mg L^{-1} $^{13}C_6$; $^{15}N_2$ L-lysine-2HCl, 84 mg L^{-1} $^{13}C_6$; $^{15}N_4$ L-arginine-HCl; 40 mg L^{-1} unlabelled L-proline) or light (146 mg L^{-1} unlabelled L-lysine-2HCl; 84 mg L^{-1} unlabelled L-arginine-HCl: 40 mg L^{-1} unlabelled L-proline) media in the presence of dialysed fetal calf serum (FCS) (v/v) (ThermoScientific, Rockford, Illinois, USA). Mon (1·5 ng mL^{-1}) was added continuously to either light- or heavy-labelled media of MonR-RH but not to Sen-RH. Both Sen-RH and MonR-RH were grown under reversed conditions with either light- or heavy-labelled media to eliminate false-positive results and to confirm that differences in protein ratios are due to variation in sensitivity against Mon. To assure incorporation of more than 95% of heavy-labelled amino acids by the parasite, complete lytic cycles were repeated twice starting by infecting the previously labelled HFF cells with 5×10^4 tachyzoites till almost complete lysis of the cells. Infected HFF cells were further incubated at 37 °C until the majority of cells were damaged after 148 h p.i. due to asexual replication of tachyzoites. Low infectious doses during passage were used to enable complete incorporation of labelled amino acids. MonR-RH was grown in the presence of Mon (1·5 ng mL^{-1}) (Treeck *et al*. 2014). Three biological replicates were used for labelling as illustrated in Fig. 1b.

Harvesting and lysis. When more than 80% of HFF cells appeared obviously damaged by tachyzoite replication, viable tachyzoites were harvested, sheared using a 25-gauge needle, and passed through filter paper (MN 640 m, Carl Roth GmbH, Germany). Tachyzoites were counted using a haemocytometer and their number was standardized in all replicates to 8×10^7 tachyzoites/replicate. All replicates were washed twice with ice-cold PBS (1×). Cell lysate was prepared by resuspending cell pellets in 300 μL lysis buffer (6 M urea, 2 M thiourea, 100 mM ammonium bicarbonate and 10 mM DTT) and incubated at room temperature for 5 min. Protease inhibitor cocktail (Complete Mini, EDTA-free, Roche, Germany) was added to the lysis buffer. Cell debris and non-dissolved material were removed by centrifugation (16 000 ***g***, 18 °C, 10 min). Protein concentration was determined for each sample by Pierce 660 nm assay (Thermo Fisher Scientific, USA) using bovine serum albumin as standard (Sigma-Aldrich, Germany). A 12·5 μg of each heavy-labelled replicate was mixed with an equal amount of its corresponding light-labelled replicate.

One-dimensional sodium dodecyl sulphate-polyacrylamide gel electrophoresis (SDS-PAGE). Protein precipitation of each biological replicate was performed with pre-chilled acetone (−20 °C) overnight, followed by centrifugation (16 000 ***g***, 18 °C, 10 min) and concentration (30 °C, 5 min) using concentrator plus (Eppendorf, Germany). Total protein was separated using 12% SDS-PAGE as described before (Brunelle and Green, 2014) and stained with Coomassie blue for 1 min. Each gel line was cut in four gel pieces and slices of each part were subjected to different reaction tubes.

In-gel digestion. In-gel reduction, alkylation and destaining of proteins were performed as previously described (Georgieva *et al*. 2008). In-gel digestion was performed by adding trypsin from bovine pancreas (1 : 50 per slice, i.e. 100 ng per 5 μg protein, Roche, Germany) and incubated overnight at 37 °C. Digestion was stopped by adding formic acid [final concentration 1% (v/v)]. Peptides were eluted with 50% (v/v) acetonitrile containing 0·1% (v/v) formic acid. Eluates were combined with the supernatant and dried by vacuum centrifugation. Samples were reconstituted with 0·1% (v/v) formic acid for LC-MS/MS analysis.

https://doi.org/10.1017/S0031182017001512 Published online by Cambridge University Press

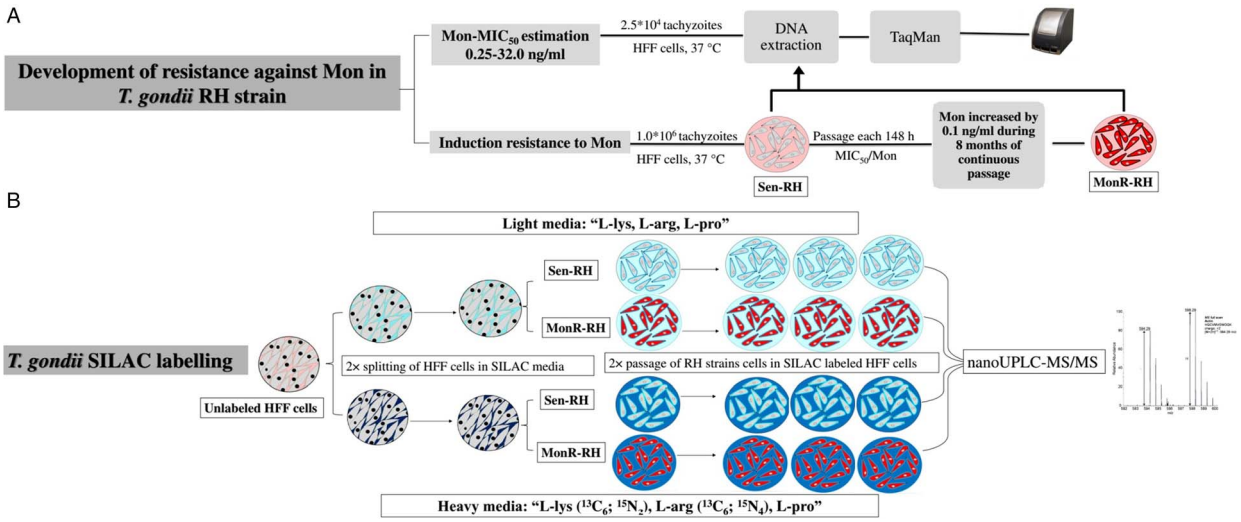

Fig. 1. Experimental flowchart: (a) Induction of resistance against Mon in *Toxoplasma gondii* RH strain, (b) SILAC labelling for comparison between Sen-RH and MonR-RH *T. gondii* strains.

nanoUPLC-MS/MS analysis

The measurements were performed as described earlier (Schmidt *et al*. 2016).

In brief, for labelled samples, 5 μL of each peptide solution was injected into the Dionex UltiMate 3000 RSLCnano system (ThermoScientific). The peptides were flushed with 2% ACN, 0·05% trifluoroacetic acid (v/v) on an Acclaim PepMap 100 column (75 μm × 2 cm, C18, Thermo Scientific) for 3 min. Peptide separation was conducted by reversed phase LC on an Acclaim PepMap 100 column (75 μm, 25 cm, C18, ThermoScientific) by use of solvents A [0·1% FA (v/v)] and B [80% ACN (v/v), 0·08% FA (v/v)]. The 90 min gradient was set as follows: constant 4% B for 3 min, increase to 30% B for 45 min, increase to 55% B for 12 min. Thereafter, the column was flushed with up to 99% B for 10 min and equilibrated to 4% B for 20 min. The separated peptides were ionized by a chip-based electrospray device (TriVersa NanoMate ion source, Advion, Ithaca, New York, USA) at a voltage of 1·7 kV. MS full scans were conducted using Q Exactive HF (ThermoScientific) at $R = 60\,000$ setting the AGC target to 5×10^6 and the maximum injection time to 150 ms. The 10 most abundant ions exceeding a threshold of $2{\cdot}5 \times 10^4$ were selected for fragmentation by higher energy C-trap dissociation at a normalized collision energy of 28. MS/MS scans were conducted at $R = 15\,000$ setting the AGC target to 2×10^5 and the maximal injection time to 80 ms. The dynamic exclusion for MS/MS scans was set to 30 s. MS/MS peak lists were generated by Xcalibur software (version 3·0, ThermoScientific).

Peptide and protein identification and quantification

MS/MS-data analysis was conducted using the Proteome Discoverer software (version 2.1, ThermoScientific) as described elsewhere (Schmidt *et al*. 2016). The acquired data were searched against the corresponding databases of *T. gondii* (all proteins in Uniprot knowledgebase, 67 674 sequence entries, 16 August 2016) in target and decoy mode using the integrated Sequest HT search algorithm. The following search parameters were used: mass tolerance for precursor ions was set to 10 ppm and for fragment ion to 0·5 Da, respectively; two missed cleavages were allowed setting trypsin in specific mode; carbamidomethylation of cysteine was set as static modification, whereas oxidation of methionine and deamidation of asparagine and glutamine were set as dynamic modifications. The false discovery rate (FDR) for peptide spectrum matches (PSMs) and peptide identifications were set to 0·01. Identified proteins needed to contain at least one unique peptide and the FDR was set to 0·05. For quantification, the default method 'SILAC 2plex (Arg10, Lys8)' was used. If not stated otherwise the default parameters of the software were used.

Data analysis

For MIC_{50} determination of Mon required to inhibit *T. gondii* (RH strain), dose–response curve was plotted using non-linear regression fitted with least squares method. For comparison between Sen-RH and MonR-RH in growth rates and % of Kolmogorov–Smirnov test of the data did not confirm normal distribution of data. Therefore, Kruskal–Wallis and Mann–Whitney *U* tests were used to evaluate the data. GraphPad Prism® 5·0 (Version 5.01, GraphPad Software, Inc., La Jolla, CA, USA) was used to generate the dose–response curve and SPSS statistic 22® (IBM, New York, 2014) was used for statistical comparison between Sen-RH and MonR-RH.

https://doi.org/10.1017/S0031182017001512 Published online by Cambridge University Press

All abundance ratios gained from proteomic experiment were log2-transformed and median normalized to zero. To be considered as significantly regulated, a protein needed to be quantified in at least five of six replicates with a mean log2-fold change (FC) >0·5 or <–0·5 and a P value <0·05 (Student's t-test, two-tailed, unpaired).

Protein classifications are based on terms retrieved from the Proteome Discoverer software-integrated ProteinCenter Annotations workflow node. The protein enrichment analysis was performed using R (R Development Core Team, 2011) and the *enricher* function of the package clusterProfiler (PMID: 22455463). Therefore, the gene ontology (GO) IDs of all identified proteins were retrieved from the Uniprot Knowledgebase. Enriched GO IDs within the group of regulated proteins were searched against the background of all identified proteins.

RESULTS

Induction of Mon resistance in RH strain

The ability of Sen-RH tachyzoites to replicate under exposure to Mon at concentrations ⩾2 ng mL^{-1} was significantly reduced with >98·0% inhibition, whereas 0·25 and 0·5 ng mL^{-1} of Mon resulted in 11·9% and 68·8% inhibition after 72 h, respectively (Fig. 2a). The dose–response curve estimated 0·4 ng mL^{-1} Mon as MIC_{50} (Fig. 2b). However, concentration of 0·5 ng mL^{-1} Mon supplemented medium was determined for selective induction of resistance by continuous passaging of Sen-RH tachyzoites. Based on daily observations of intracellular tachyzoite development by light microscopy, the Mon dose was gradually increased. Additionally, qPCR assays were used before increasing Mon concentration to confirm microscopic evaluation of tachyzoite replication as described earlier (Edvinsson *et al.* 2006). After 8 months of passaging under Mon exposure, a resistant strain (MonR-RH) that can grow in continuous presence of higher Mon concentrations (2·0 ng mL^{-1}) was obtained. Despite the ability of MonR-RH to grow in the presence of Mon, daily microscopic observation revealed that its ability to destroy HFF cells completely was delayed (148 h) in comparison with Sen-RH (96 h p.i.) using $1{\cdot}0 \times 10^6$ tachyzoites as initial infectious dose. Because of that, comparison between both strains in growth rate and % of inhibition was performed 96 h p.i. instead of 72 h p.i. in MIC determination of Sen-RH. Growth rate of Sen-RH was significantly ($P < 0{\cdot}05$) higher compared with MonR-RH in non-treated controls, while there was no significant difference in the presence of 0·5, 1·0 and 2·0 ng mL^{-1} Mon. MonR-RH grew significantly ($P < 0{\cdot}05$) higher compared with Sen-RH in the presence of 3·0 and 4·0 ng mL^{-1} Mon (Fig. 3).

There was no significant difference in the % of replication between Sen-RH and MonR-RH in the

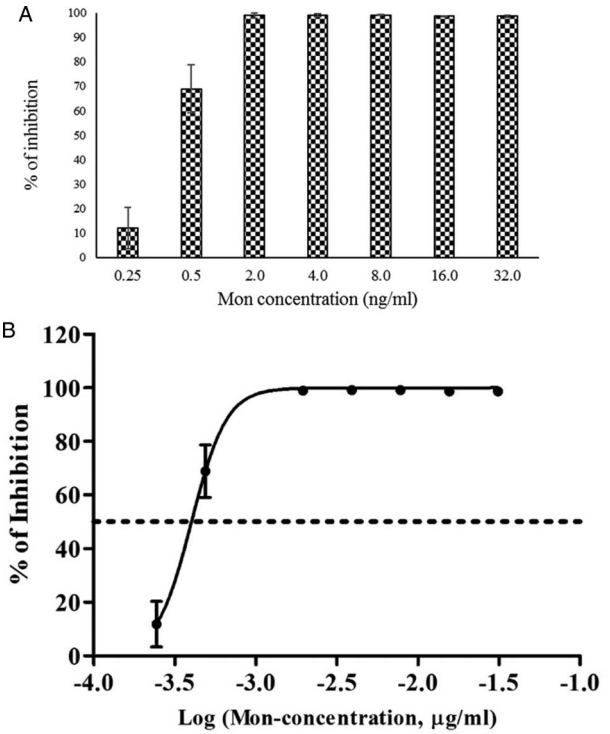

Fig. 2. *In vitro* MIC_{50} estimation of Sen-RH *Toxoplasma gondii* tachyzoites. (a) Per cent (%) of inhibition after 72 h incubation in HFF cells with different concentrations of Mon (0·25–32 ng mL^{-1}), *gene copy numbers were significantly lower in Mon treated groups (>0·5 ng mL^{-1}) compared with infected, non-treated control ($P < 0{\cdot}05$). (b) The dose–response curve estimated 0·4 ng mL^{-1} Mon as MIC_{50}.

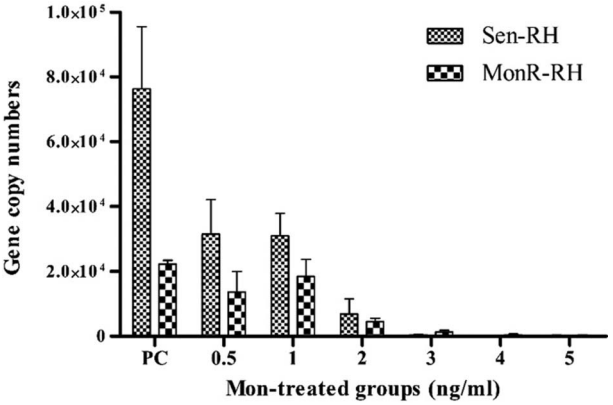

Fig. 3. Comparison of *in vitro* growth rate (gene copy numbers) between Sen-RH and MonR-RH tachyzoites in the absence (positive control; PC) or presence of different Mon concentrations (ng mL^{-1}) after 96 h incubation in HFF cells. *Growth rate was significantly higher in PC of Sen-RH compared with presence of Mon. †Growth rate was significantly higher in PC of MonR-RH compared with the presence of Mon at concentrations >2·0 ng mL^{-1}. ●Growth rate was significantly higher in Sen-RH compared with MonR-RH. #Growth rate was significantly higher in MonR-RH compared with Sen-RH, $P < 0{\cdot}05$.

https://doi.org/10.1017/S0031182017001512 Published online by Cambridge University Press

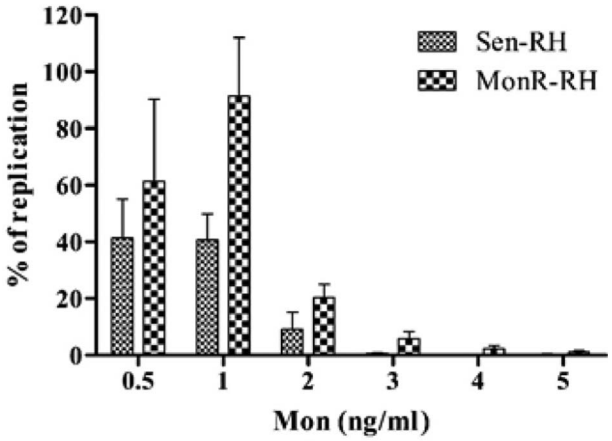

Fig. 4. Comparison of *in vitro* per cent of replication between Sen-RH and MonR-RH tachyzoites in the presence of different Mon concentrations (0·5–5 ng mL^{-1}) after 96 h incubation in HFF cells.

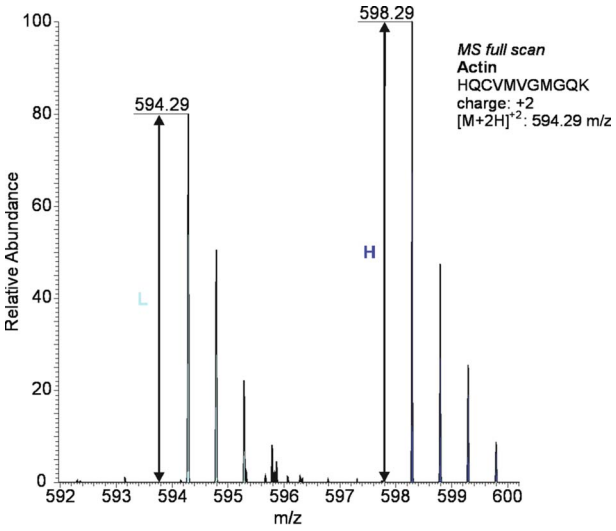

Fig. 5. An illustrative example of protein quantification using SILAC: actin protein was significantly ($P < 0·05$) upregulated in Mon-resistant strain of *Toxoplasma gondii* (MonR-RH) compared with sensitive parental strains (Sen-RH): the lower-mass peak clusters (○) are from light labelled arg/lys peptides of Sen-RH, while higher mass peak clusters (●) are from heavy labelled arg/lys peptides of MonR-RH.

presence of 0·5 ng mL^{-1} Mon. However, MonR-RH could grow in the presence of 2·0 ng mL^{-1} Mon with a replication rate of 20·3% after 96 h of cultivation in comparison to 9·0% for the parental Sen-RH strain, while its replication rate was 91·4% in the presence of 1·0 ng mL^{-1} Mon. Replication rate of MonR-RH compared with Sen-RH was significantly ($P <$ 0·05) higher in concentrations >0·5 ng mL^{-1} Mon (Fig. 4).

Proteomic comparison of T. gondii *strains (Sen-RH and MonR-RH) using SILAC*

Both *T. gondii* Sen-RH and MonR-RH tachyzoites were successfully grown and passaged in the presence or absence of labelled amino acids. |Overall, 1820 proteins were identified by at least one unique peptide (online Supplementary Table S1) in at least one biological replicate. Among the total identified proteins, 1024 proteins were relatively quantified in more than four biological replicates (e.g. actin; Fig. 5) and 52 regulated proteins were found in significantly different quantities between Sen-RH and MonR-RH [FC <–0·5 or >0·5 (*t*-test significance value $P < 0·05$)]. Regulated proteins in MonR-RH compared with Sen-RH were either upregulated (42 proteins) or downregulated (10 proteins) (Fig. 6a, Table 1). All regulated proteins were classified based on either their cellular component or molecular function. The majority of these proteins either play a role in metabolism, protein synthesis (catalytic activity) or were uncharacterized proteins (Fig. 6b). However, a protein enrichment analysis revealed proteins being involved in GTP binding (GO:0005525) and small GTPase mediated signal transduction (GO:0007264) as significantly enriched among the group of regulated proteins ($P < 0·01$, online Supplementary Table S2). All proteins assigned to these terms were significantly upregulated, including the co-atomer γ subunit, Rab6 and the GTPase RAB7, both known for their vesicular transporter activity. All identified proteins were cross-checked for entries in the ToxoDB and the corresponding IDs were included to online Supplementary Table S1. However, only 41 out of all 1024 identified proteins could be assigned to proteins from the ToxoDB. Since the initial protein identification process was based on the usage of all *T. gondii* protein entries from the Uniprot knowledgebase, a missing assignment in the ToxoDB could also be due to an insufficient ID mapping. The upload of the dataset to the ToxoDB is planned.

Actin and β-tubulin cofactor D are known to play a role in cellular transport of *T. gondii* tachyzoites during invasion process (Takemae *et al*. 2013). Both actin and the putative β-tubulin cofactor D were significantly ($P < 0·01$) upregulated in MonR-RH. Sixteen proteins were annotated as membrane proteins and most of them were upregulated in MonR-RH. Microneme membrane protein 8 (MIC8), which is a coccidian surface protein related to the respective apical organelle that plays a role in host cell invasion (Cérède *et al*. 2005), was downregulated. Cathepsin CPL (protein synthesis) and a putative transmembrane protein were also downregulated in MonR-RH. Putative metalloproteinase TNL4 and MIC8 proteins were functionally classified as metal ion-binding proteins and both were downregulated. Perforin-like protein (PLP1) is a cell surface protein that is found in the apical area and was downregulated in MonR-RH (Table 2).

https://doi.org/10.1017/S0031182017001512 Published online by Cambridge University Press

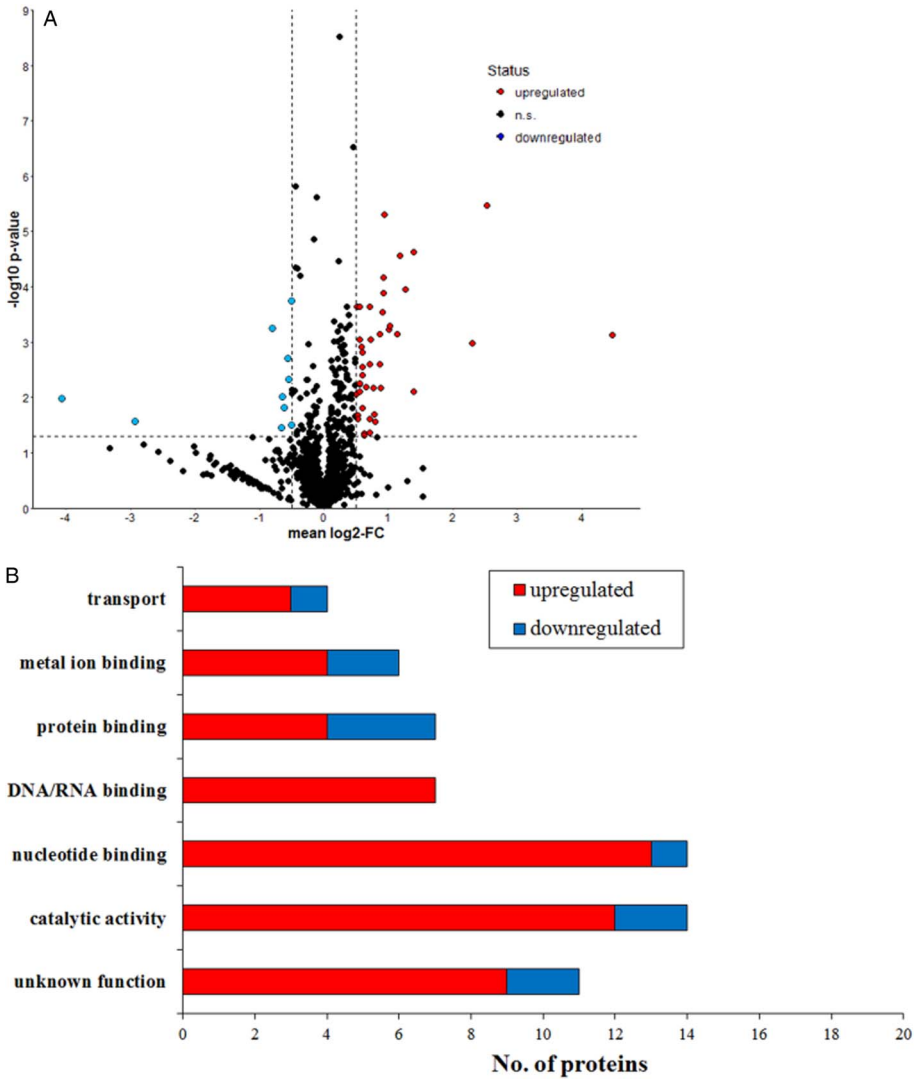

Fig. 6. Relatively quantified proteins between MonR-RH and Sen-RH (a) Volcano plot of all quantified proteins. The dotted lines indicate threshold set for regulation: FC <−0·5 or >0·5 and the *t*-test significance value ($P < 0·05$). (b) Red bars indicate higher expression of MonR-RH in comparison with Sen-RH, whereas blue bars indicate lower expression.

Table 1. Total number of proteins identified and quantified in MonR-RH and Sen-RH *Toxoplasma gondii* strains (regulated proteins were quantified in at least five of six replicates)

	MonR-RH *vs* Sen-RH strains
Total proteins identified (FDR <0·05)	1820
Proteins quantified	1024
Regulated proteins	52 (5·1%)
Upregulated	42 (4·1%)
Downregulated	10 (1·0%)

DISCUSSION

In *T. gondii* RH strain, resistance against various anticoccidials was induced by continuous *in vitro* growth in the presence of sub-lethal concentrations of these drugs (Ricketts and Pfefferkorn, 1993). Because similar drug targets in apicomplexan parasites can be assumed, selection of Mon resistance in *T. gondii* can provide insights into putative general mechanisms of resistance that also apply to *E. tenella*. Furthermore, induction of *in vitro* resistance against Mon in *T. gondii* RH strain tachyzoites allows controlled conditions and reduces variation. We used this as a selective reference model for polyether ionophores resistance in coccidia.

We firstly established an *in vitro* model to induce Mon resistance in *T. gondii* (RH strain). After multiple passages, offspring tolerated Mon at a concentration of 2 ng mL^{-1}, whereas the estimated MIC_{50} for the parental strain (Sen-RH) was 0·4 ng mL^{-1}. However, development of MonR-RH was slower as manifested by increased time needed to complete lysis of HFF cells (148 h p.i.) and detection of lower gene copy numbers in the absence of Mon (96 h p.i.) in comparison with Sen-RH.

https://doi.org/10.1017/S0031182017001512 Published online by Cambridge University Press

Table 2. Functional classification of regulated proteins between MonR-RH and Sen-RH of *Toxoplasma gondii*

Accession no.	Protein description	Log2-FC	S.D.	*t*-test *P* value	Cellular component	Molecular function
Upregulated proteins (arranged based on *t*-test *P* value)						
S8EUX3	Uncharacterized protein	2·53	0·56	3·46E-06		
A0A086PTS5	SAG-related sequence SRS35B	0·94	0·22	4·93E-06		
A0A086M999	Elongation factor Tu	1·39	0·42	2·37E-05		RNA binding; cell cycle; catalytic activity; nucleotide binding
B9QA65	Putative vacuolar protein sorting-associated protein vps4	1·18	0·36	2·72E-05		RNA binding; cell cycle; catalytic activity; nucleotide binding
A0A086PM49	Ulp1 protease family, C-terminal catalytic domain-containing protein	0·93	0·32	6·89E-05		Catalytic activity
A0A086K649	Putative β-tubulin cofactor D	1·27	0·43	1·12E-04		Protein binding; enzyme regulator activity
A0A086KQ45	Uncharacterized protein	0·92	0·34	1·30E-04		
A0A086JG41	SAG-related sequence SRS17B	0·56	0·22	2·29E-04	Membrane	
A0A086Q8V2	Ribosomal-ubiquitin protein RPL40	0·71	0·28	2·31E-04	Ribosome	Protein binding; catalytic activity; structural molecule activity
A0A0F7V4F1	Serine/threonine-protein phosphatase	0·51	0·21	2·33E-04		Metal ion binding; catalytic activity
A0A086KYU9	Putative rhoptry protein	0·91	0·35	2·89E-04	Membrane	
A0A086M6B0	Putative translation initiation factor IF-2	1·03	0·46	5·09E-04		RNA binding; cell cycle
S7VNC9	Actin protein	1·01	0·46	5·99E-04		Nucleotide binding; cellular transport
S8FZ63	Co-atomer γ subunit	0·87	0·4	7·06E-04	Membrane	Transporter activity
A0A086LQ23	Uncharacterized protein	1·13	0·53	7·30E-04		
S7UKA0	SAG-related sequence SRS13 1	4·48	1·99	7·38E-04	Membrane	
A0A086JI47	Enoyl-CoA hydratase/isomerase family protein	0·55	0·26	8·91E-04		Catalytic activity
A0A086QHG3	Putative calmodulin	0·73	0·35	8·96E-04		
A0A125YJX4	SAG-related sequence SRS16B	2·3	1·13	1·03E-03	Membrane	
A0A0F7V0E9	26S protease regulatory subunit 6b/putative	0·58	0·29	1·22E-03	Cytoplasm	RNA binding; cell cycle; catalytic activity; nucleotide binding
A0A086QHJ5	GTPase RAB7	0·6	0·31	1·56E-03	Membrane	Transporter activity: nucleotide binding
A0A086LVM4	Putative ATP-dependent RNA helicase DDX1	0·87	0·49	2·48E-03		Protein binding; nucleotide binding
S7WA24	S1 RNA binding domain-containing protein	0·71	0·39	2·52E-03	Membrane	
A0A086J913	Putative small GTPase Rab2	0·59	0·34	2·88E-03	Membrane	Nucleotide binding; cellular transport; cellular communication
A0A086JFP3	Uncharacterized protein	0·59	0·34	4·03E-03		
A0A086JJ89	Putative eukaryotic peptide chain release factor	0·56	0·34	5·67E-03	Cytoplasm	RNA binding; cell cycle
A0A086JV56	Putative small GTP binding protein rab1a	0·55	0·35	5·81E-03	Membrane	Nucleotide binding; cellular transport; cellular communication
A0A086JYQ2	Putative dense granule protein GRA12	0·65	0·41	6·43E-03		
A0A151H876	DEAD/DEAH box helicase domain-containing protein (fragment)	0·88	0·56	6·81E-03		
A0A086K0T3	Putative transmembrane protein	0·77	0·49	6·89E-03	Membrane	

https://doi.org/10.1017/S0031182017001512 Published online by Cambridge University Press

Table 2. (*Cont.*)

Accession no.	Protein description	Log2-FC	S.D.	*t*-test *P* value	Cellular component	Molecular function
A0A151H1H8	SAG-related sequence SRS19D	1·39	0·9	7·93E-03		
I7CBG7	Rhoptry kinase family protein	0·55	0·37	8·02E-03		Nucleotide binding; cellular transport; catalytic activity
A0A125YQA8	Rhoptry protein ROP18	0·5	0·35	8·96E-03		Nucleotide binding; cellular transport; catalytic activity
A0A086QZR3	Rab6 protein	0·6	0·44	1·55E-02	Membrane	Transporter activity; nucleotide binding
A0A125YSM0	Histone H3	0·78	0·63	2·03E-02	Chromosome/ nucleus	Protein binding; DNA binding
A0A086L9J8	Uncharacterized protein	0·53	0·44	2·13E-02		
A0A151H0P7	Ras family protein	0·71	0·58	2·45E-02		
A0A086JC72	SAG-related sequence protein SRS22E	0·53	0·45	2·49E-02	Membrane	
A0A0F7UWG8	CAM kinase, CDPK family	0·79	0·68	2·81E-02		Metal ion binding; catalytic activity; nucleotide binding
A0A086KIF9	Mitogen-activated protein kinase	0·71	0·67	4·31E-02		Nucleotide binding; cellular transport; signal transducer activity
A0A086PWP8	Putative transmembrane protein	0·62	0·59	4·50E-02	Membrane	
A0A086JCV3	RuvB-like helicase	0·62	0·62	4·79E-02	Nucleus	Nucleotide binding; cellular transport; catalytic activity
Downregulated proteins (arranged based on *t*-test *P* value)						
A0A086LBS4	Putative pre-folding subunit 6	−0·51	0·19	1·85E-04		Protein binding
A0A086LYQ6	Perforin-like protein PLP1	−0·81	0·37	5·76E-04	Membrane/ apical organelle	
A0A086JQA0	Uncharacterized protein	−0·55	0·29	1·94E-03		
A0A125YJZ7	Microneme protein MIC8	−0·54	0·34	4·86E-03	Membrane/ apical organelle	Metal ion binding; protein binding
A0A086JQN8	Cathepsin CPL	−0·65	0·46	9·75E-03	Membrane	Catalytic activity
A0A086MAR0	Putative transmembrane protein	−4·08	2·83	1·08E-02	Membrane	
F1DI03	Putative metalloproteinase TLN4	−0·63	0·48	1·56E-02		Metal ion binding
S7UXD1	3-hydroxyisobutyrate dehydrogenase	−2·94	2·57	2·81E-02		Nucleotide binding; cellular transport; catalytic activity
A0A0F7V2K0	RNA binding protein/ putative	−0·51	0·44	3·17E-02		Nucleotide binding; cellular transport; cell cycle
A0A086JCQ9	SRP72 RNA-binding domain-containing protein	−0·66	0·61	3·55E-02		Transporter activity; protein binding; RNA binding

Previously, SILAC was applied successfully in *T. gondii* and amino acid incorporation was confirmed to be more than 95% after four lytic cycles (i.e. 24 h) (Treeck *et al*. 2014). In our study, to assure maximal labelling with heavy amino acids, Sen-RH and MonR-RH were passaged sequentially twice in previously labelled HFF cells (i.e. each time for 148 h).

It is known that egress of merozoites from the host cell is triggered by elevated cytosolic calcium levels in apicomplexan organisms after ionophore treatment (Caldas *et al*. 2007), which could be a major antiparasitic effect of ionophores. The anticoccidial modes of action and resistance mechanisms were extensively studied; nevertheless, relevant gaps in knowledge still exist. Mon and maduramicin drug-resistant lines of *E. tenella* were compared with their sensitive parental lines using cDNA arrays and suggested that mechanisms of resistance might be very complex (Chen *et al*. 2008).

https://doi.org/10.1017/S0031182017001512 Published online by Cambridge University Press

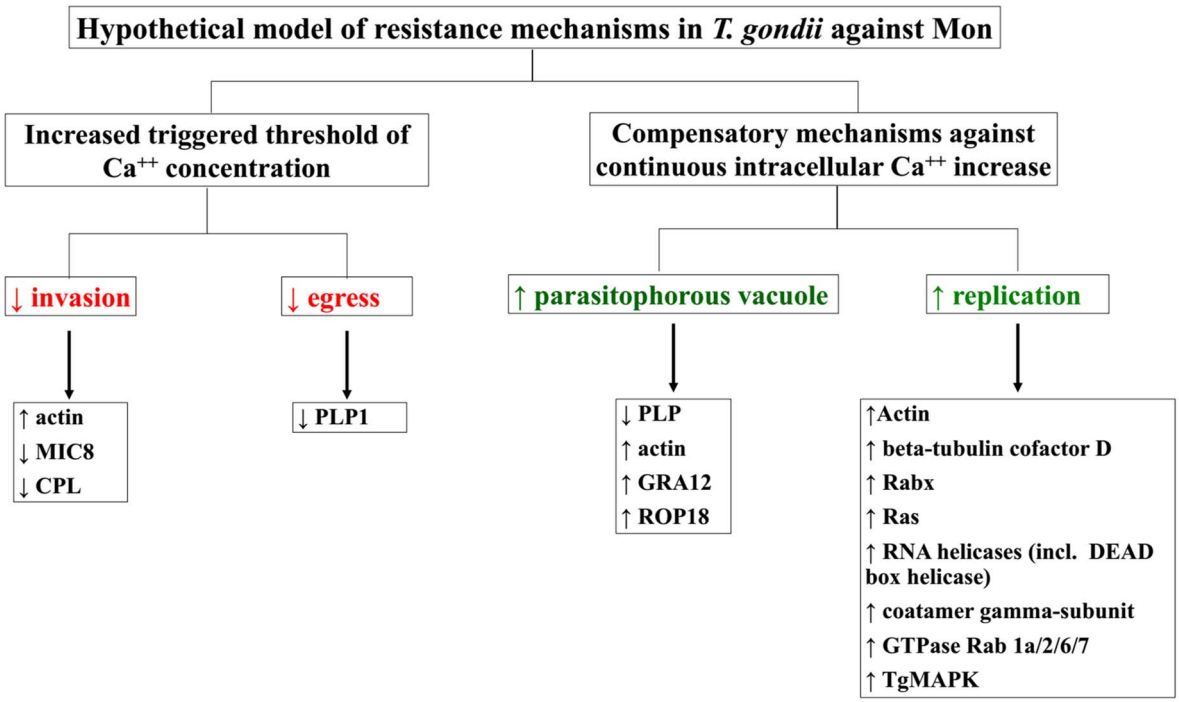

Fig. 7. A schematic summary of resistance mechanisms in MonR-RH *Toxoplasma gondii* strain against Mon (red marks indicates decrease while green marks increase of respective life cycle phase).

Resistance against Mon was previously generated by induced mutation in *T. gondii*. In this mutant strain, mitochondrial MutS DNA damage repair enzyme (TgMSH-1) was selectively suppressed. Despite the decreased sensitivity towards Mon in TgMSH-1, retard invasion ability in comparison with parental strain was detected (Garrison and Arrizabalaga, 2009). Furthermore, a disruption in cell cycle of *T. gondii* was considered an important mediator of sensitivity towards polyether ionophores (Lavine and Arrizabalaga, 2011). MutS domain-containing protein (S7UY47) was identified in the current study but not quantified (two out of six replicates). Relative protein abundances were lower in MonR-RH compared with Sen-RH in both replicates (data not shown), which is in accordance with the previously described role of MSH in resistance to polyether ionophores.

Several proteins that were significantly up- or downregulated were identified in MonR-RH. Among several classes of proteins (Table 2), the small GTPase-mediated signal transduction could be identified as specifically and significantly enriched among the regulated proteins. Moreover, several mechanistic pathways were altered in the resistant compared with the parental RH strain. The regulated proteins could be grouped into proteins with major involvement in different events during the parasitic life cycle.

Interestingly, the results of *T. gondii* SILAC analysis indicate changes in the parasite activity related to invasion, egress, forming of the parasitophorous vacuole (PV) and replication. It seems that invasion and egress are reduced while intracellular replication is enhanced in the MonR-RH strain compared with the Sen-RH parental strain. A summary of the suggested aspects of resistance in MonR-RH strain is illustrated in Fig. 7.

Actin, a conserved microfilament protein, was upregulated in MonR-RH compared with Sen-RH. Actin plays an important role in host cell invasion by conoid extrusion (Del Carmen *et al.* 2009) and in replication. It is found beneath the parasitic cell membrane in clusters (Dobrowolski *et al.* 1997), mainly localized at the apical end of *T. gondii* tachyzoites (Song *et al.* 2004). It could be shown that actin participates actively in irreversible calcium-induced conoid extrusion during ionophore treatment (Mondragón and Frixione, 1996; Del Carmen *et al.* 2009). Thus, the observed increase in actin in resistant strains may be linked to higher resistance to calcium-mediated structural dysfunction, induced primarily by the Na^+-ionophore Mon.

Apicomplexan invasion mechanisms basically rely on secretion of microneme, rhoptry and dense granule proteins (Tardieux and Baum, 2016). Observed invasion-associated changes in resistant MonR-RH include a significant reduction in microneme protein MIC8. MIC8 is described as essential factor during invasion by forming a tight interaction (moving junction) between contents of micronemes and the host cell (Kessler *et al.* 2008). In *T. gondii*, MIC8 is mainly found in tachyzoites and serves as transporter (escorter protein) for MIC2-associated protein (Rabenau *et al.* 2001). MIC8 was firstly considered as an escorter/transporter for soluble

https://doi.org/10.1017/S0031182017001512 Published online by Cambridge University Press

adhesion MIC3 (Meissner *et al*. 2002) but then Kessler *et al*. (2008) demonstrated that MIC8 and MIC3 are part of the same complex and that this function might be redundant. MIC3 (A0A086LPW4; online Supplementary Table S1) was slightly decreased in MonR-RH compared with Sen-RH; however, this reduction was not significant. Downregulation in MIC2 was also detected in a sulfadiazine-resistant *T. gondii* strain (ME49), which corresponds with our results (Doliwa *et al*. 2013). In addition, cathepsin L-like cysteine protease (TgCPL) expression was reduced. TgCPL is considered as an important protein for invasion and replication due to its role in maturation of MIC, protein degradation, i.e. in the PV, and in endolysosomes (Dou and Carruthers, 2011; Liu *et al*. 2014). Decrease of both proteins (MIC8 and TgCPL) in resistant strains under Mon exposure can be interpreted as a correlate for lower invasion activity.

However, several proteins that are linked to intracellular PV structure and parasite replication were upregulated. GRA12 localizes in the PV and seems to be involved in the formation of the membranous nanotubular network (MNN). The MNN is supposed to allow a higher exchange rate between host cell and parasites inside the PV, thus triggering parasite development, and affecting the structural organization of daughter cells within the PV (Travier *et al*. 2008). An increase of GRA12 expression is assumed to be related to a stronger or faster genesis of the MNN. GRA12 is expressed mainly by tachyzoites and sporozoites and to a lesser extent by dormant bradyzoites (Mercier and Cesbron-Delauw, 2015) and reflects high intracellular parasite replication in MonR-RH-infected cells. The assumption of an activated parasite replication is supported by the observed upregulation of the cytosolic and vesicular parasite proteins actin and calmodulin (co-localized, supporting, i.e. the transport of dense granules; Heaslip *et al*. 2016), β-tubulin cofactor D (crucial for the assembly of functional β-tubulin; Fedyanina *et al*. 2009) and co-atomer γ-subunit (supporting general vesicle coating including presence in the apical complex; Smith *et al*. 2007). Interestingly, this coincides with the increase of GTPases (Rabx, Ras) that are essential for intracellular vesicle transport and regulation of the cytoskeleton (Field *et al*. 1999) substantiating the assumption of functional alterations and structural upregulation – i.e. higher intracellular replication – in the Mon-resistant parasite population. Moreover, significant enrichment of GTP binding and GTPase-mediated signal transduction proteins supports their role in enhancing replication. In *Plasmodium berghei*, it has been found that the ionophores nigericin and Mon, as well as NH_4Cl, can increase cytosolic Ca^{++} (Luo *et al*. 1999). These reviews suggest a possible mechanism of reducing cytosolic Ca^{++} through activation of different membrane trafficking proteins, such as actin, coatomer and RAB proteins.

ROP18 is known as a virulence factor mediating the parasite evasion from host cell immune response of interferon-inducible p47-GTPase (Khaminets *et al*. 2010). The observed ROP18 increase corresponds to a higher resistance of MonR-RH to adverse effects, i.e. by the host cell.

While several changes regarding replication were elucidated, which indicate parasite activation, some hints to stage conversion could also be noticed. Several helicases including the DEAD box helicase were uniformly upregulated. Previously, it was shown that upregulation of DEAD box helicase occurs generally during cellular stress and translational arrest by assembling of the cytoplasmic RNA stress granules, which might seem plausible in MonR-RH under Mon exposure (Cherry and Ananvoranich, 2014). The mitogen-activated protein kinase (TgMAPK-1) has been found to be stress-activated (Brumlik *et al*. 2004), but also to accumulate during stage conversion into bradyzoites.

We observed significant upregulation of several SAG-related sequences (SRS) partly known to be expressed by bradyzoites (Wasmuth *et al*. 2012; Pittman *et al*. 2014), i.e. SRS16B and SRS13, which showed the highest increase. This indicates a higher production of dormant stages. This thesis is corroborated by low expression of the perforin-like protein PLP1, which was shown to be essentially involved in PV rupture, parasite egress and host cell lysis (Roiko and Carruthers, 2013; Borges-Pereira *et al*. 2015). Additionally, the aforementioned decrease in TgCPL expression supports this hypothesis because it suggests reduced host cell protein digestion in endolysosomes of resistant protozoa. This is indicative for a higher proportion of dormant and metabolic less active stages, and could represent beginning conversion of a subpopulation into bradyzoites.

The precise factors that regulate the relationship between intracellular replication and conversion to dormant bradyzoites are still unclear. However, Dzierszinski *et al*. (2004) stated that increased intracellular replication might occur in early dormant stages. Moreover, factors that control conversion from active to dormant stages and vice versa in *T. gondii* are rather constitutive and based on the same mechanisms (Hu *et al*. 2002).

To summarize the findings in *T. gondii* experiments, we observed a slower host cell lysis by the parasite in MonR-RH compared with the parental Sen-RH. This finding can be linked with the proteomic characterization of both strains. In connection with Mon resistance, MonR-RH developed a lower invasion and egress activity, which might indicate an increase in the triggered threshold of Ca^{++} concentration needed to induce egress. The replication activity and integrity of PV seem to be increased in

https://doi.org/10.1017/S0031182017001512 Published online by Cambridge University Press

MonR-RH, which might be a compensation process to provide enough surrogates for a significant proportion of killed parasites, which does not occur in the parental strain. Normally, egress is triggered by Mon (Caldas *et al*. 2007). Obviously, the resistant strain developed a mechanism to counterbalance this process by (partial) inactivation of replicated parasites. Invasion and egress are selectively reduced while a triggered replication resulting in a consistently higher number of intracellular stages. This allows for parasite multiplication and invasion of host cells on a lower but sufficient level under Mon exposure. A validation of our suggested model of resistance against Mon should address selected regulated proteins (e.g. MIC8) to evaluate their role in resistance development towards Mon. Further characterization of MonR-RH in comparison with Sen-RH will enable determining whether these proteomic changes are in line with the previously described knock out of TgMSH-1 or whether different types of resistance exist.

CONCLUSION

Induction of resistance against Mon resulted in lower growth rates in MonR-RH compared with parental Sen-RH. By SILAC-based MS/MS analyses, several differences between Mon-resistant and non-resistant strains could be demonstrated. Higher availability of actin and downregulation of microneme proteins (MIC8) were found, which might indicate their major role in establishing resistance towards Mon. It is concluded that resistance is not a simple process but is expressed by reduced invasion and egress activity while intracellular replication is enhanced. In *T. gondii*, there are multiple hints for resistance-associated metabolic changes indicating an increase of dormant stages (bradyzoites). The suggested model of resistance mechanisms in coccidia against Mon has to be confirmed by other methods like standard invasion and lysis assays, Western blot and immunofluorescent assays to proof our interpretation for validity.

SUPPLEMENTARY MATERIAL

The supplementary material for this article can be found at https://doi.org/10.1017/S0031182017001512.

ACKNOWLEDGEMENT

We would like to thank Maj Schuster for excellent technical assistance.

FINANCIAL SUPPORT

Ahmed Thabet was supported by DAAD (German Academic Exchange Service) Deutscher Akademischer Austauschdienst, grant no. 91540992.

CONFLICT OF INTEREST

Authors declare no conflict of interest.

REFERENCES

Borges-Pereira, L., Budu, A., McKnight, C., Moore, C., Vella, S., Triana, M., Liu, J., Garcia, C., Pace, D. and Moreno, S. (2015). Calcium signaling throughout the *Toxoplasma gondii* lytic cycle. A study using genetically encoded calcium indicators. *The Journal of Biological Chemistry* **290**, 26914–26926.

Brumlik, M. J., Wei, S., Finstad, K., Nesbit, J., Hyman, L. E., Lacey, M., Burow, M. E. and Curiel, T. J. (2004). Identification of a novel mitogen-activated protein kinase in *Toxoplasma gondii*. *International Journal of Parasitology* **34**, 1245–1254.

Brunelle, J. L. and Green, R. (2014). One-dimensional SDS-polyacrylamide gel electrophoresis (1D SDS-PAGE). *Methods in Enzymology* **541**, 151–159.

Caldas, L. A., de Souza, W. and Attias, M. (2007). Calcium ionophore-induced egress of *Toxoplasma gondii* shortly after host cell invasion. *Veterinary Parasitology* **147**, 210–220.

Cérède, O., Dubremetz, J., Soête, M., Deslée, D., Vial, H., Bout, D. and Lebrun, M. (2005). Synergistic role of micronemel protein in *Toxoplasma gondii* virulence. *The Journal of Experimental Medicine* **201**, 453–463.

Chapman, H. D., Jeffers, T. K. and Williams, R. B. (2010). Forty years of monensin for the control of coccidiosis in poultry. *Poultry Science* **89**, 1788–1801.

Chen, T., Zhang, W., Wang, J., Dong, H. and Wang, M. (2008). *Eimeria tenella*: analysis of differentially expressed genes in the monensin- and maduramicin-resistant lines using cDNA array. *Experimental Parasitology* **119**, 264–271.

Cherry, A. A. and Ananvoranich, S. (2014). Characterization of a homolog of DEAD-box RNA helicases in *Toxoplasma gondii* as a marker of cytoplasmic mRNP stress granules. *Gene* **543**, 34–44.

Couzinet, S., Dubremetz, J. F., Buzoni-Gatel, D., Jeminet, G. and Prensier, G. (2000). *In vitro* activity of the polyether ionophorous antibiotic monensin against the cyst form of *Toxoplasma gondii*. *Parasitology* **121**, 359–365.

Del Carmen, M. G., Mondragón, M., González, S. and Mondragón, R. (2009). Induction and regulation of conoid extrusion in *Toxoplasma gondii*. *Cellular Microbiology* **11**, 967–982.

Dobrowolski, J. M., Niesman, I. R and Sibley, L. D. (1997). Actin in the parasite *Toxoplasma gondii* is encoded by a single copy gene, ACT1 and exists primarily in a globular form. *Cell Motility and the Cytoskeleton* **37**, 253–262.

Doliwa, C., Xia, D., Escotte-Binet, S., Newsham, E. L., Sanya, J. S., Aubert, D., Randle, N., Wastling, J. M. and Villena, I. (2013). Identification of differentially expressed proteins in sulfadiazine resistant and sensitive strains of *Toxoplasma gondii* using difference-gel electrophoresis (DIGE). *International Journal of Parasitology: Drugs and Drug Resistance* **3**, 35–44.

Dou, Z. and Carruthers, V. B. (2011). Cathepsin proteases in *Toxoplasma gondii*. *Advances in Experimental Medicine and Biology* **712**, 49–61.

Dubey, J. P., Velmurugan, G. V., Rajendran, C., Yabsley, M. J., Thomas, N. J., Beckmen, K. B., Sinnett, D., Ruid, D., Hart, J., Fair, P. A., McFee, W. E., Shearn-Bochsler, V., Kwok, O. C. H., Ferreira, L. R., Choudhary, S., Faria, E. B., Zhou, H., Felix, T. A. and Su, C. (2011). Genetic characterisation of *Toxoplasma gondii* in wildlife from North America revealed widespread and high prevalence of the fourth clonal type. *International Journal of Parasitology* **41**, 1139–1147.

Dzierszinski, F., Nishi, M., Ouko, L. and Roos, D. (2004). Dynamics of Toxoplasma gondii differentiation. *Eukaryotic cell* **3**, 992–1003.

Edvinsson, B., Lappalainen, M. and Evengård, B., ESCMID Study Group for Toxoplasmosis. (2006). Real-time PCR targeting a 529-bp repeat element for diagnosis of toxoplasmosis. *Clinical Microbiology and Infection* **12**, 131–136.

Fedyanina, O. S., Book, A. J. and Grishchuk, E. L. (2009). Tubulin heterodimers remain functional for one cell cycle after the inactivation of tubulin-folding cofactor D in fission yeast cells. *Yeast* **26**, 235–247.

Field, M. C., Ali, B. R. and Field, H. (1999). GTPases in protozoan parasites: tools for cell biology and chemotherapy. *Parasitology Today* **15**, 365–371.

Garrison, E. and Arrizabalaga, G. (2009). Disruption of a mitochondrial MutS DNA repair enzyme homologue confers drug resistance in the parasite *Toxoplasma gondii*. *Molecular Microbiology* **72**, 425–441.

Georgieva, D., Risch, M., Kardas, A., Buck, F., von Bergen, M. and Betzel, C. (2008). Comparative analysis of the venom proteomes of *Vipera ammodytes* and *Vipera ammodytes* meridionalis. *Journal of Proteome Research* **7**, 866–886.

Heaslip, A. T., Leung, J. M., Carey, K. L., Catti, F., Warshaw, D. M., Westwood, N. J., Ballif, B. A. and Ward, G. E. (2010). A small-molecule inhibitor of *T. gondii* motility induces the posttranslational modification of myosin light chain-1 and inhibits myosin motor activity. *PLoS Pathogens* **6**, e1000720.

Heaslip, A. T., Nelson, S. R. and Warshaw, D. M. (2016). Dense granule trafficking in *Toxoplasma gondii* requires a unique class 27 myosin and actin filaments. *Molecular Biology of the Cell* **27**, 2080–2089.

Hu, K., Mann, T., Striepen, B., Beckers, C., Roos, D. and Murray, J. (2002). Daughter cell assembly in the protozoan parasite *Toxoplasma gondii*. *Molecular Biology of the Cell* **13**, 593–606.

Kessler, H., Herm-Götz, A., Hegge, S., Rauch, M., Soldati-Favre, D., Frischknecht, F. and Meissner, M. J. (2008). Microneme protein 8 – a new essential invasion factor in *Toxoplasma gondii*. *Journal of Cell Science* **121**, 947–956.

Kevin, D. A., Meujo, D. A. and Hamann, M. T. (2009). Polyether ionophores: broad-spectrum and promising biologically active molecules for the control of drug-resistant bacteria and parasites. *Expert Opinion on Drug Discovery* **4**, 109–146.

Khaminets, A., Hunn, J. P., Könen-Waisman, S., Zhao, Y. O., Preukschat, D., Coers, J., Boyle, J. P., Ong, Y. C., Boothroyd, J. C., Reichmann, G. and Howard, J. C. (2010). Coordinated loading of IRG resistance GTPases on to the *Toxoplasma gondii* parasitophorous vacuole. *Cellular Microbiology* **12**, 939–961.

Lavine, M. D. and Arrizabalaga, G. (2011). The antibiotic monensin causes cell cycle disruption of *Toxoplasma gondii* mediated through the DNA repair enzyme TgMSH-1. *Antimicrobial Agents and Chemotherapy* **55**, 745–755.

Liu, J., Pace, D., Dou, Z., King, T. P., Guidot, D., Li, Z. H., Carruthers, V. B. and Moreno, S. N. (2014). A vacuolar-H(+)-pyrophosphatase (TgVP1) is required for microneme secretion, host cell invasion, and extracellular survival of *Toxoplasma gondii*. *Molecular Microbiology* **93**, 698–712.

Luo, S., Marchesini, N., Moreno, S. N. and Docampo, R. (1999). A plant-like vacuolar H(+)-pyrophosphatase in *Plasmodium falciparum*. *FEBS Letters* **460**, 217–220.

Mavin, S., Joss, A., Ball, J. and Ho-Yen, D. O. (2004). Do *Toxoplasma gondii* RH strain tachyzoites evolve during continuous passage?. *Journal of Clinical Pathology* **57**, 609–611.

McFarland, M. M., Zach, S. J., Wang, X., Potluri, L. P., Neville, A. J., Vennerstrom, J. L. and Davis, P. H. (2016). A review of experimental compounds demonstrating anti-*Toxoplasma* activity. *Antimicrobial Agents and Chemotherapy* **20**, 7017–7034.

Meissner, M., Reiss, M., Viebig, N., Carruthers, V. B., Toursel, C., Tomavo, S., Ajioka, J. W. and Soldati, D. (2002). A family of transmembrane microneme proteins of *Toxoplasma gondii* contain EGF-like domains and function as escorters. *Journal of Cell Science* **115**, 563–574.

Mercier, C. and Cesbron-Delauw, M. F. (2015). *Toxoplasma* secretory granules: one population or more?. *Trends in Parasitology* **31**, 60–71.

Mondragón, R. and Frixione, E. (1996). Ca (2+)-dependence of conoid extrusion in *Toxoplasma gondii* tachyzoites. *Journal of Eukaryotic Microbiology* **43**, 120–127.

Ong, S. E. and Mann, M. (2005). Mass spectrometry-based proteomics turns quantitative. *Nature Chemical Biology* **1**, 252–262.

Peek, H. W. and Landman, W. J. M. (2003). Resistance to anticoccidial drugs of Dutch avian *Eimeria* spp. field isolates originating from 1996, 1999 and 2001. *Avian Pathology* **32**, 391–401.

Pittman, K. J., Aliota, M. T. and Knoll, L. J. (2014). Dual transcriptional profiling of mice and *Toxoplasma gondii* during acute and chronic infection. *BMC Genomics* **15**, 806.

R Development Core Team (2011). *R: A Language and Environment for Statistical Computing*. The R Foundation for Statistical Computing, Vienna, Austria. ISBN: 3-900051-07-0. Available online at http://www.R-project.org/.

Rabenau, K. E., Sohrabi, A., Tripathy, A., Reitter, C., Ajioka, J. W., Tomley, F. M. and Carruthers, V. B. (2001). TgM2AP participates in *Toxoplasma gondii* invasion of host cells and is tightly associated with the adhesive protein TgMIC2. *Molecular Microbiology* **41**, 537–547.

Ricketts, A. P. and Pfefferkorn, E. R. (1993). *Toxoplasma gondii*: susceptibility and development of resistance to anticoccidial drugs *in vitro*. *Antimicrobial Agents and Chemotherapy* **37**, 2358–2363.

Roiko, M. S. and Carruthers, V. B. (2013) Functional dissection of *Toxoplasma gondii* perforin-like protein 1 reveals a dual domain mode of membrane binding for cytolysis and parasite egress. *The Journal of Biological Chemistry* **288**, 8712–8725.

Schmidt, J., Kliemt, S., Preissler, C., Moeller, S., von Bergen, M., Hempel, U. and Kalkhof, S. (2016). Osteoblast-released matrix vesicles, regulation of activity and composition by sulfated and non-sulfated glycosaminoglycans. *Molecular and Cellular Proteomics* **15**, 558–572.

Smith, S. S., Pfluger, S. L., Hjort, E., McArthur, A. G. and Hager, K. M. (2007). Molecular evolution of the vesicle coat component betaCOP in *Toxoplasma gondii*. *Molecular Phylogenetics and Evolution* **44**, 1284–1294.

Song, H. O., Ahn, M. H., Ryu, J. S., Min, D. Y., Joo, K. H. and Lee, Y. H. (2004). Influence of calcium ion on host cell invasion and intracellular replication by *Toxoplasma gondii*. *Korean Journal of Parasitology* **42**, 185–193.

Stephan, B., Rommel, M., Daugschies, A. and Haberkorn, A. (1997). Studies of resistance to anticoccidials in *Eimeria* field isolates and pure *Eimeria* strains. *Veterinary Parasitology* **69**, 19–29.

Takemae, H., Sugi, T., Kobayashi, K., Gong, H., Ishiwa, A., Recuenco, F., Murakoshi, F., Iwanaga, T., Inomata, A., Horimoto, T., Akshi, H. and Kato, K. (2013). Characterization of the interaction between *Toxoplasma gondii* rhoptry neck protein 4 and host cellular β-tubulin. *Scientific Reports* **13**, 3199.

Tardieux, I. and Baum, J. (2016). Reassessing the mechanics of parasite motility and host-cell invasion. *The Journal of Cell Biology* **214**, 507–515.

Travier, L., Mondragon, R., Dubremetz, J. F., Musset, K., Mondragon, M., Gonzalez, S., Cesbron-Delauw, M. F. and Mercier, C. (2008). Functional domains of the *Toxoplasma* GRA2 protein in the formation of the membranous nanotubular network of the parasitophorous vacuole. *International Journal of Parasitology* **38**, 757–773.

Treeck, M., Sanders, J. L., Gaji, R. Y., LaFavers, K. A., Child, M. A., Arrizabalaga, G., Elias, J. E. and Boothroyd, J. C. (2014). The calcium-dependent protein kinase 3 of *Toxoplasma* influences basal calcium levels and functions beyond egress as revealed by quantitative phosphoproteome analysis. *PLoS Pathogens* **10**, e1004197.

Wasmuth, J. D., Pszenny, V., Haile, S., Jansen, E. M., Gast, A. T., Sher, A., Boyle, J. P., Boulanger, M. J., Parkinson, J. and Grigg, M. E. (2012). Integrated bioinformatic and targeted deletion analyses of the SRS gene superfamily identify SRS29C as a negative regulator of Toxoplasma virulence. *MBio Journal* **3**, pii: e00321-12.

Wu, L., Zhang, Q. X., Li, T. T., Chen, S. X. and Cao, J. P. (2009). [*In vitro* culture of *Toxoplasma gondii* tachyzoites in HFF and HeLa cells]. *Zhongguo Ji Sheng Chong Xue Yu Ji Sheng Chong Bing Za Zhi* **27**, 229–231.

https://doi.org/10.1017/S0031182017001512 Published online by Cambridge University Press